Available online at www.sciencedirect.com
ScienceDirect
Ceramics International 33 (2007) 1463–1468
CERAMICS INTERNATIONAL
www.elsevier.com/locate/ceramint

Effect of citric acid on the synthesis of nano-crystalline yttria stabilized zirconia powders by nitrate–citrate process

K.A. Singh [a], L.C. Pathak [b,*], S.K. Roy [a]

[a] *Department of Metallurgical and Materials Engineering, Indian Institute of Technology, Kharagpur 721302, India*
[b] *National Metallurgical Laboratory, Jamshedpur 831007, India*

Received 16 February 2006; received in revised form 17 March 2006; accepted 17 May 2006
Available online 25 September 2006

Abstract

The role of citric acid on the preparation of nano-crystalline cubic YSZ powder using a citrate–nitrate solution combustion technique is reported. Thermo-gravimetric analyses reveal that the exothermic peak of nitrate–citrate redox reaction disappears with the increase in citric acid content. The crystallite size of the cubic YSZ powder initially increases with the increase in citric acid content and then decreases upon further addition of citric acid. Particle coarsening has been found to significantly increase upon increase in calcination temperature from 650 °C (11.1 nm) to 800 °C (65.3 nm). Transmission electron microscopic studies in conjunction with XRD analyses indicate a low degree of agglomeration in the synthesized powder. Microwave heating of the solution can control the particle size and yield c-YSZ powder having sizes ~15 nm.

Keywords: Nitrate–citrate; Combustion synthesis; TG/DTA; TEM study; YSZ and nano-crystalline ceramics

1. Introduction

Pure zirconia exhibits three well-defined polymorphs under atmospheric pressure, with monoclinic, tetragonal and cubic symmetries and also has an orthorhombic phase at high pressure [1]. Zirconia has high melting point (~2700 °C), low thermal conductivity, high ionic conductivity and excellent mechanical, high hardness, high elastic modulus, low coefficient of friction, low wear resistance, good chemical and interesting electrical properties [2,3]. The different phases of ZrO_2 exhibit their own intrinsic physical and chemical properties. The high volume expansion during phase transformation from monoclinic to tetragonal restricts its widespread use in the ceramic industry. To overcome this, stable cubic or tetragonal phases at room temperature are desirable and efforts are being made to lower the temperature range of stability of these phases by the use of different dopants such as MgO, CaO, Y_2O_3, Sc_2O_3, Mg_3N_2, Si_3N_4, AlN, etc. [4–8]. The content of these dopants determines whether the stabilized phase will be tetragonal or cubic. Stabilized cubic zirconia has a fluorite structure and exhibits considerable ionic conductivity at elevated temperatures making the material electrically conductive due to the migration of oxygen vacancies introduced by the stabilizer [9]. Stabilized c-ZrO_2 is specially used in oxygen sensors [10], solid oxide fuel cells [9,11], ceramic components and as catalyst or catalyst promoters in synthesis of alcohol by hydrogenation of CO [7].

Recently, the nano-structured zirconia based ceramic powders are gaining importance and various routes have been employed for the production of nano-crystalline zirconia-based particles, such as co-precipitation [12], sol–gel preparation method [13], hydrothermal synthesis [14,15], polymerized complex processes [16] and gel-combustion process [5,6,8,12,17,18]. The gel-combustion process seems to be quite simple, does not involve multiple steps and it is more versatile compared with the other solution routes and yields high surface area products of desired composition having excellent sinterability. Being a solution process, atomic level doping and excellent control of stoichiometric homogeneity can be achieved in the gel-combustion method and it is relatively less costly than alkoxide-based sol–gel methods. Gel-combustion routes are based on the gelling and subsequent combustion of a solution containing salts of the desired metals (usually nitrates) and some organic fuels, such as urea [18], carbo-hydrazide [19], citric acid [8,20], glycine [21], etc.

* Corresponding author. Tel.: +91 657 43 1752; fax: +91 657 42 6527.
E-mail address: lokesh@nmlindia.org (L.C. Pathak).

0272-8842/$32.00
doi:10.1016/j.ceramint.2006.05.021

Though the gel-combustion technique using citrate–ammonia route has been studied widely, very little literature is available on the various aspects of this process. Amongst them, the pH of the solution, temperature and composition of the solution are important. The reported gel-combustion technique using citrate–ammonia route [5,8] used metal nitrates as the oxidant of redox reaction that on combustion yield NO_x, which is not environment friendly. The role of citric acid content on the combustion synthesis of nano-crystalline ZrO_2 + 8 mol% of Y_2O_3 powder by a citrate–nitrate combustion technique has been investigated and the pertinent results are discussed. In this present investigation, we have intentionally used small amount of metal nitrates in the form of $Y(NO_3)_3$ to carry out the combustion reaction with less emission of NO_x gases.

2. Experimental

A simple and versatile process that utilizes a chemical pyrophoric reaction to yield ultra fine ceramic powders has been adopted to prepare nano-crystalline cubic-yttria stabilized zirconia (c-YSZ) powder. In this process, a clear solution was prepared by dissolving 10.7 g of $ZrOCl_2{\cdot}8H_2O$ in about 50 ml of distilled water. Subsequently, the required amount (8 mol%) of Y_2O_3, i.e. 0.565 g was dissolved in dilute HNO_3 upon heating. Both the solutions were mixed to prepare 125 ml stock solution of $ZrOCl_2{\cdot}8H_2O$ with 8 mol% of Y_2O_3 (0.25 M). This final solution was equally divided into five parts to which 0, 2, 5, 10 and 15 g of citric acid monohydrate ($C_6H_8O_7{\cdot}H_2O$) were added to vary the citrate content. The pH of all the solutions was adjusted to 8 by adding liquor ammonia and the resulting solutions were heated on a hot plate (to ~300 °C). An extra sample containing 10 g of citric acid (CA) was heated inside a microwave oven. Apart from the solution, which contained no citric acid, all other solutions turned into black and viscous gels, which upon continued heating swelled up forming fine flakes with the evolution of gases, yielding foamy voluminous masses. The solution without citric acid first formed a transparent viscous gel, which on continued heating turned into a white powder. Subsequently, the as-prepared powders were calcined at two different temperatures viz. 650 and 800 °C for a period of 1 h. The process has been schematically shown in Fig. 1.

The dried semi-solid gel type of mass collected prior to decomposition was investigated by a thermal analyzer (TG/DSC, TA Instruments, USA), where an equal amount of high purity α-Al_2O_3 powder was used as the reference. Both the test and the reference samples were heated at a rate of 10 °C/min during TG/DSC measurements. Subsequently, the as-prepared and the calcined powder were characterized by powder X-ray diffraction technique using Ni-filtered Co Kα radiation with the help of an XRD analyzer (Siemens, Germany). The prepared powders were also characterized by transmission electron microscopy (TEM, CM-200, Phillips Netherlands). Carbon coated grids were used to support the ultrasonically dispersed calcined powder for the TEM observations.

Particle sizes were calculated from the line broadening of the X-ray diffraction peaks using the Scherrer formula. For

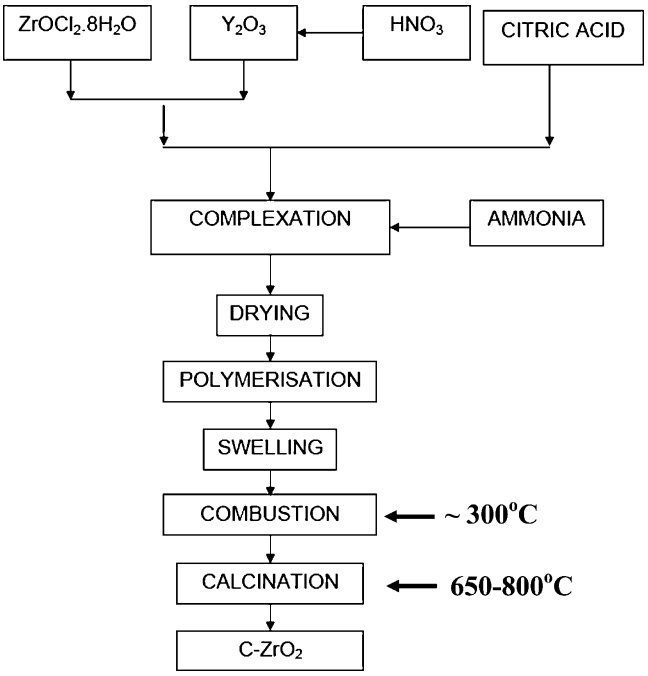

Fig. 1. Schematic flow diagram of the nitrate–citrate process.

calculation of correct line broadening, XRD analysis of polycrystalline graphite having crystallite size more than 100 μm was used to measure the instrumental line broadening, which was found out to be 0.46° at the diffraction peak angle of 31°. Corrected line broadening, θ_{corr} was calculated using the following formula:

$$\theta_{corr} = (\theta_o^2 - \theta_i^2)^{1/2} \quad (1)$$

where θ_o and θ_i are the values of observed and instrumental line broadening, respectively. The lattice parameter "*a*" of the c-YSZ was calculated using the following equation:

$$a = d(h^2 + k^2 + l^2)^{1/2} \quad (2)$$

where "*h k l*" are the miller indices of the plain of diffraction and "*d*" is the inter planer spacing. Graphite powder (99.9% pure) was used as the internal standard for the estimation of lattice parameters.

3. Results and discussion

The solution containing zirconium oxy-chloride-(yttrium nitrate)-citric acid-ammonia, upon heating transforms into a semi-solid black colored gel type of mass, which on further heating swells up to yield a foamy charred mass. The DSC plots as depicted in Fig. 2 for the various samples show that the nature of the reactions changes with the variation in citric acid content of the solution. It is quite evident that the ratio of citrate to nitrate ions (c/n) plays a significant role on the exothermicity of the reactions. The DSC plot in Fig. 3 shows an exothermic peak at 260 °C for the sample with a citric acid content of 2 g. In this case, the exothermic heat generated in the combustion technique is governed by the thermally induced redox reaction

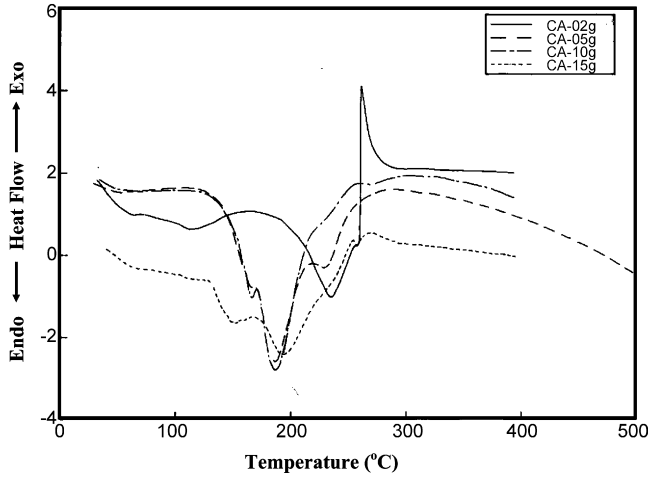

Fig. 2. DSC plots of the precursor gels made with various amount of citric acid.

involving citrate and nitrate anions present in the precursor, where, the nitrate ions acts as oxidant and citrate ions acts as reductant. The combustion wave propagates from one point to the end point of the reactant and the combustion reaction is complete within a few seconds. With the addition of NH_4OH to the solution $ZrO(OH)_2$ forms by the following reaction.

$$ZrO(Cl)_2 + 2NH_4OH \rightarrow ZrO(OH)_2 + 2NH_4Cl. \quad (3)$$

The $ZrO(OH)_2$ particles remain colloidally dispersed in the presence of citrate in the solution. According to the concepts employed in propellant chemistry, the exothermic redox reactions (citrate–nitrate) that proceed during the synthesis is written as [22]:

$$18Y(NO_3)_3 + 15C_6H_8O_7 \rightarrow 90CO_2 + 27N_2 + 60H_2O + 9Y_2O_3. \quad (4)$$

Though the amount of nitrate ions in the solution is less, the redox mixture generates sufficient exothermic heat for the calcination of the precursors into metal oxides and produces a large amount of gases in a short period of time that keeps the powder well dispersed in large volume. The exothermic heat decompose the $ZrO(OH)_2$ to ZrO_2 and H_2O by the following reaction.

$$ZrO(OH)_2 \rightarrow ZrO_2 + H_2O. \quad (5)$$

It is evident from the DSC plots in Fig. 2 that as the citric acid (CA) content is increased the exothermic peak gets replaced by the endothermic peak, which clearly indicates the total disappearance of exothermicity of the reaction. Similar observation was reported by Marinsek et al. [17], where they found the decrease of exothermicity as the composition got farther away from the stoichiometric c/n ratio of 0.28. In the present investigation, the amount of citrate ions was very high (reductant) compared to the nitrate ions (oxidant), as much less amount of HNO_3 was used to prepare the $Y(NO_3)_3$ solution. This resulted in insufficient amount of nitrate ions being present for carrying out the oxidation of citrate ions. Therefore, instead of the formation of the products through an exothermic reaction between the citrate–nitrate ions, the reaction shifts over to a simple decomposition of the oxy-chloride salts (Eq. (5)). Simple decomposition of Y-nitrate is endothermic and is accompanied by the evolution of acidic NO_2 gas:

$$4Y(NO_3)_3 \rightarrow 2Y_2O_3 + 12NO_2 + 3O_2. \quad (6)$$

The origin of the endothermic peaks in the DSC curves can be attributed to the simple decomposition of the salts along with the decomposition of citric acid. As reported by Pathak et al. [20], during heating, citric acid melts at 173 °C and converts to aconitic acid by the reaction:

$$C_6H_8O_7 \rightarrow C_6H_6O_6 + H_2O(g). \quad (7)$$

The aconitic acid then yields itaconic acid ($C_5H_6O_4$ and CO_2) on further heating. The itaconic acid (mp 166 °C), which upon continued heating undergoes polymerization and swells up resulting in de-carboxylation releasing CO_2. This polymeric matrix provides a very large volume for the dispersion of the products and results in the formation of nano-crystalline YSZ particles upon calcination. Since all the organic materials and ammonia related compounds are either volatilized or burnt off

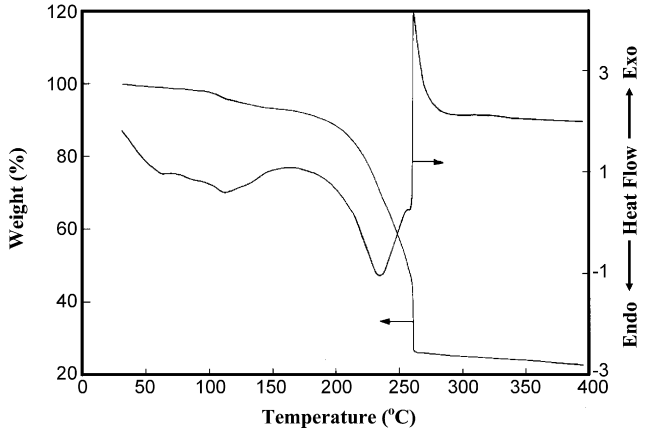

Fig. 3. TGA/DSC plot of the precursor gel with citric acid content of 2 g.

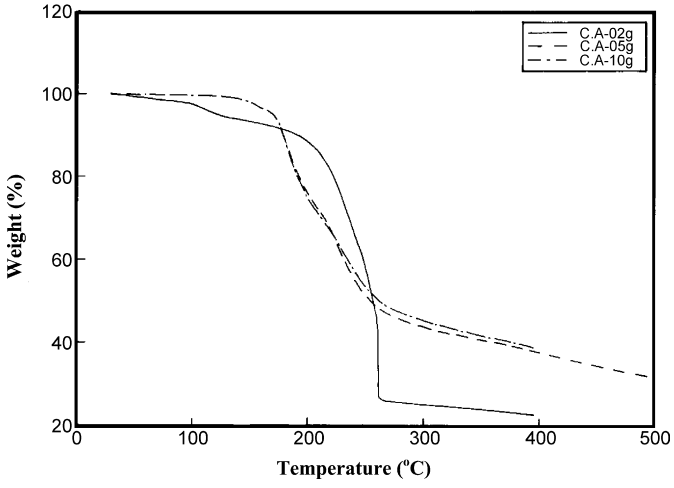

Fig. 4. TGA plots of the precursor gels made with varying citric acid.

during calcination at elevated temperatures, the purity of the YSZ powder is controlled by the purity of starting chemicals.

From the TG plots in Fig. 4, it can be observed that the decomposition of the samples with a high citrate ratio is associated with slow rate of weight loss during heating as compared to the decomposition of the sample containing 2 g of citric acid, which decomposes rapidly due to the exothermic redox reaction that has taken place in the system. Whereas, the TG plots for the other samples show sluggish weight loss due to the decreased exothermicity.

The XRD analyses of the zirconia powders calcined at two different temperatures viz. 650 and 800 °C indicates the formation of a single-crystalline cubic phase (Fig. 5). The calculated '*d*' values match with the reported yttria stabilized cubic zirconia having a composition of $Y_{0.15}Zr_{0.85}O_{1.93}$ or $92ZrO_2{\cdot}8Y_2O_3$ phase and the lattice parameter '*a*' was estimated to be 5.14 Å [23]. The appearance of X-ray line broadening indicates the nano-crystallinity of the synthesized

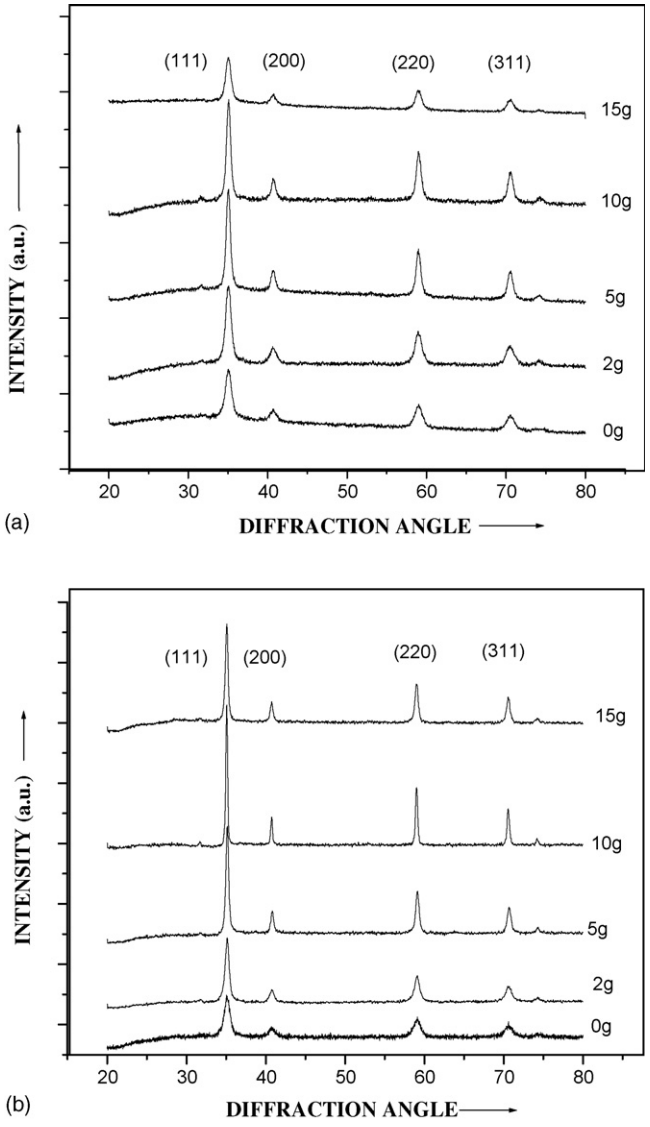

Fig. 5. XRD patterns of c-YSZ nano-powders calcined at: (a) 650 °C and (b) at 800 °C.

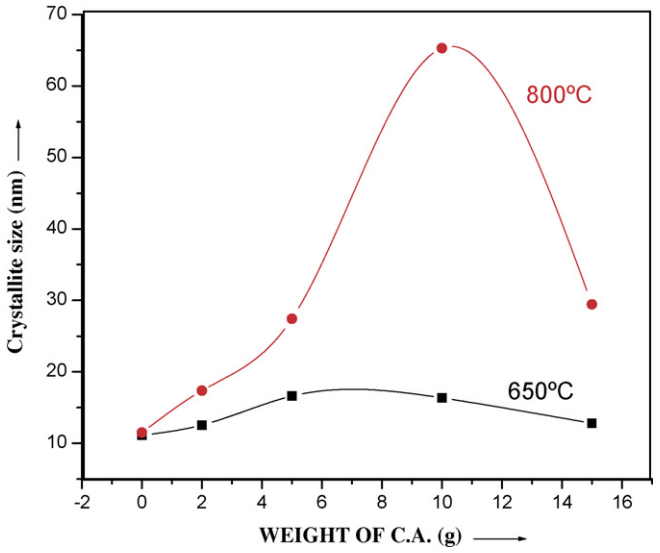

Fig. 6. Variation of crystallite size of c-YSZ powder made with varying citric acid content.

powders. The calculated crystallite (grain) sizes are plotted in Fig. 6, which shows that the crystallite (grain) sizes for the powder calcined at 650 °C initially increases of from 11.1 nm (0 g CA) to 16.6 nm (5 g CA) and then decreases to 12.8 nm (15 g CA). Upon calcination at 800 °C the grain or crystallite sizes increase to 65.3 nm for the CA content of 10 g and then decrease to 29.4 nm. This shows that the nature of the curve between crystallite size and citric acid content remains the same with the variation in the crystallite size quite distinguishable in the latter case. This is possibly due to the fact that at higher temperature nucleation rate is slow and growth rate is higher. Yang et al. demonstrated a similar variation in crystallite size with increase in fuel (citric acid) content when they had used the citrate–nitrate process for the preparation of tetragonal YSZ particles [8].

TEM micrographs as shown in Fig. 7 clearly indicate that the particle sizes of the synthesized powders are in the nano range and the particles even if agglomerated consist of fine crystallites. The selected area diffraction (SAD) of the YSZ clearly reveals the ring patterns of polycrystalline cubic zirconia phase in Fig. 8. The diffraction rings correspond to the '*d*' values of the cubic phase and the lattice parameters are in agreement with the XRD patterns. Stabilized c-ZrO_2 particles appear to be uniform in size and shapes in the TEM micrographs. Although there is a variation in particle sizes with the increase of citric acid content, there seems to be little effect on the morphology of the particles. From the TEM images (Fig. 7), the average particle size for the powder formed using 10 g of citric acid and calcined at 800 °C could be estimated as ~70 nm (Fig. 7(a)), whereas identically calcined powder made with the 5 g of citric acid addition had average particle size of ~30 nm (Fig. 7(d)). From the XRD and TEM study it has been observed that the degree of agglomeration is low in the synthesized powder, which has strong technological importance. In accordance with the XRD results, the TEM study expectedly shows the decrease of particle sizes with the

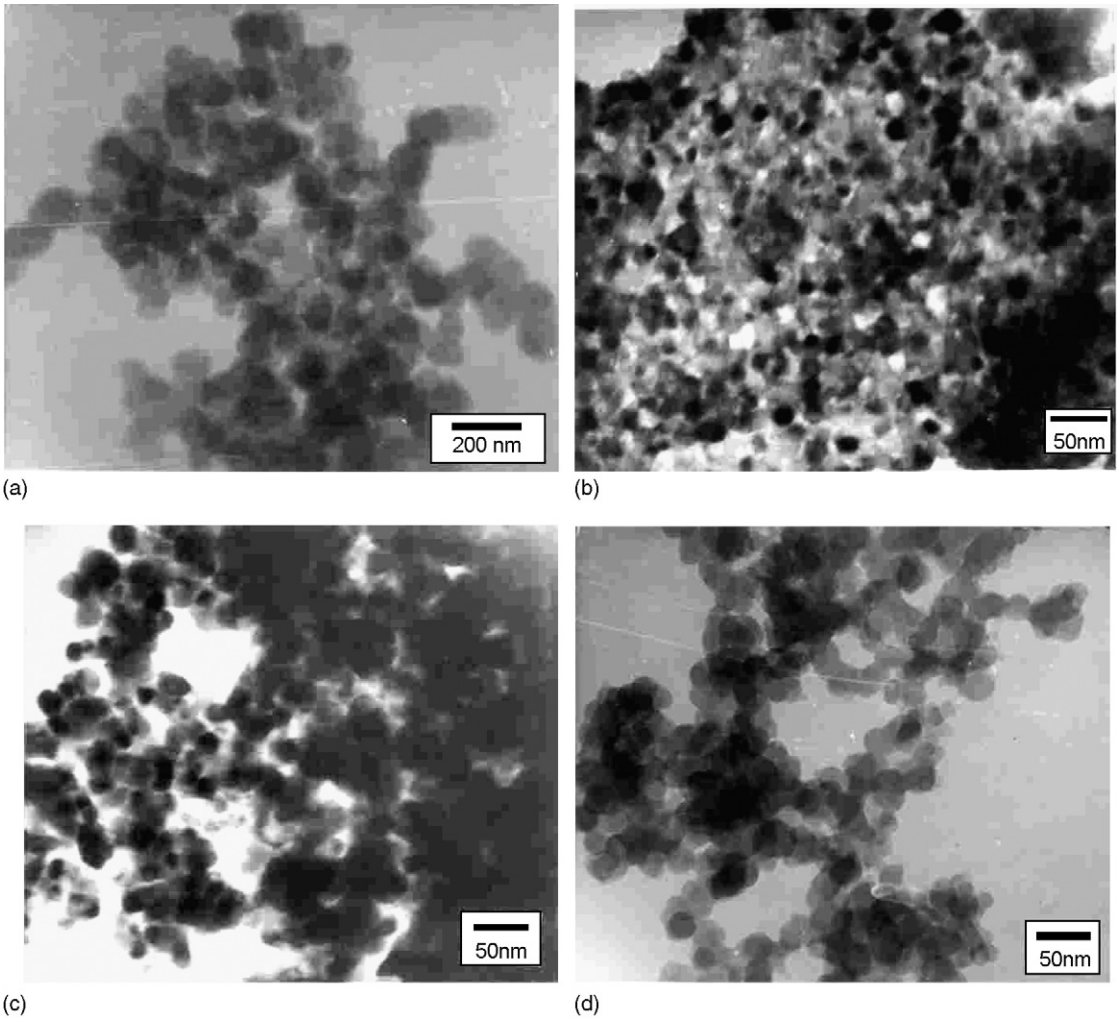

Fig. 7. TEM micrographs of c-YSZ nano-particles (a) CA = 10 g and calcined at 800 °C, (b) CA = 10 g and calcined at 800 °C, (c) CA = 10 g, microwave heated and calcined at 800 °C and (d) CA = 5 g and calcined at 800 °C.

lowering of calcination temperatures. By lowering the calcination temperature to 650 °C, the particle sizes could be reduced to 20 nm for the 10 g of citric acid added samples (Fig. 7(c)). TEM micrograph of the sample having the same citric acid content (10 g) and prepared by calcination at 800 °C after initial heating of the gel type of mass in a microwave oven shows particle size of 10–15 nm (Fig. 7(b)). Unlike on a hot plate where the source of the heat is located at the bottom only, here, in a microwave the solution is heated up uniformly through out its volume, which enables fast removal of volatile masses resulting in significant reduction in particle size.

The removal of volatile masses during calcination at elevated temperatures plays a significant role on the variation of crystallite sizes. The polymeric distribution and its subsequent removal during thermal treatment are expected to control the particle growth and the final morphology of the particles. Increase in citric acid content from 2 to 10 g (for the samples calcinated at 800 °C) results in slower decomposition of the salts and incomplete combustion of the citrate ions. Thus a lot of carbonaceous matter is left in the as-prepared powder. During calcination, the removal of gaseous products from the precursor gives rise to capillary forces on the particles, which brings more particles to come in contact with each other. This results in more particle agglomeration, cluster formation and particle growth during synthesis. Thus there is increase in particle size with the CA content. Further increase in citric acid content, as in the case of the precursor made with 15 g of CA, results in larger separation (more diffusion distance) between the zirconia particles. In this case, the presence of excess citric acid plays the role of a space-filling template and the YSZ particles embedded in polymer matrix became crystalline without interacting with other YSZ particles. This increase in the diffusion distance seems to be the actual reason for the decrease in the crystallite size upon further increase in citric acid content. Further, the reduction of crystallite sizes in microwave-heated sample having 10 g of CA clearly suggests the importance of removal of organic material during synthesis. In the microwave heating, the organic materials uniformly volatizes within a short span of time, which creates large numbers of nucleating sites. Here less synthesis time helps to control the particle sizes.

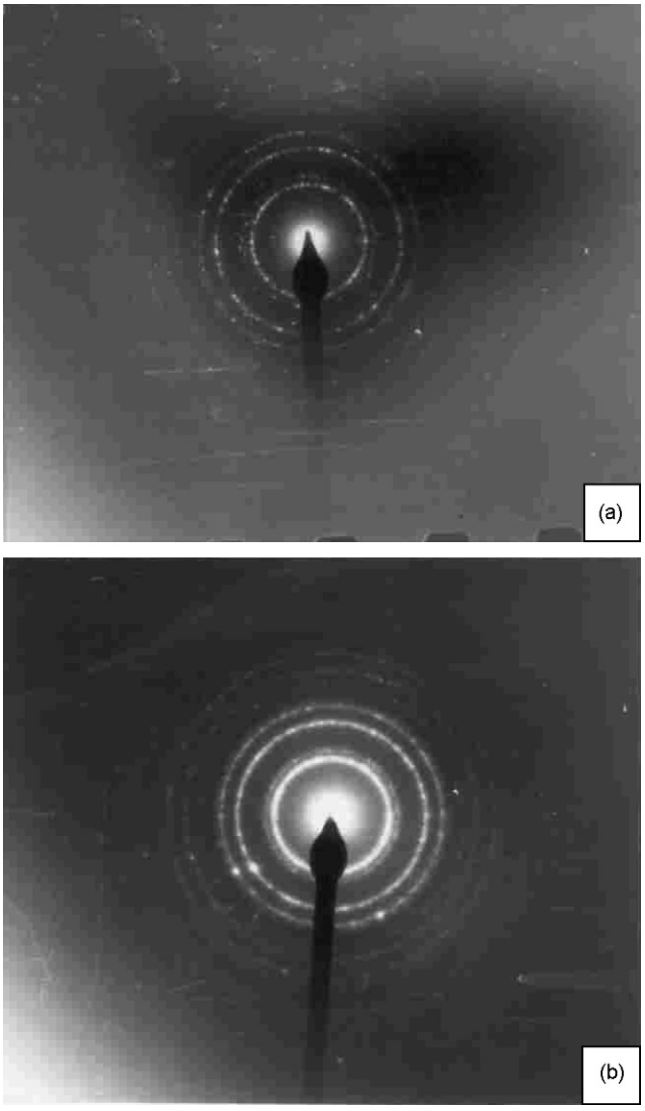

Fig. 8. SAD image of samples showing the polycrystalline c-YSZ powder made by: (a) CA = 10 g, microwave heated and calcined at 800 °C, (b) CA = 5 g and calcined at 800 °C.

4. Conclusions

A systematic investigation on the synthesis of nano-crystalline YSZ powder by a nitrate–citrate route and by varying the fuel content of the precursor solution has been carried out. With the increase of citric acid (CA) content, the exothermicity of the chemical reaction reduces and at high CA content only endothermic peaks appear in the DSC plots showing the loss of the exothermic reaction. Amount of citric acid plays an important role on the control of particle size. The crystallite size of the cubic YSZ powder initially increases with the citric acid content and then decreases. Particle coarsening becomes quite significant as the calcination temperature is increased from 650 °C (11.1 nm) to 800 °C (65.3 nm). The removal of organic species plays significant role on the size of the nano-sized c-YSZ powder. The synthesized powder shows low degree of agglomeration, which has industrial potential for scaling up. Microwave heating of the solution could control the particle size and yielded c-YSZ powder having sizes of ∼15 nm.

Acknowledgements

The authors want to thank Mr. S. Das, Mr. B. Mahato and Dr. A. Kaliath for their help in carrying out TEM, XRD and Thermal Analyses studies, respectively. The authors also want to thank Director, National Metallurgical Laboratory, Jamshedpur for his kind permission to publish this article.

References

[1] T. Chraska, A.H. King, C.C. Berndt, Mater. Sci. Eng. A 286 (2000) 169–178.
[2] R.H.J. Hannink, P.M. Kelly, B.C. Muddle, J. Am. Ceram. Soc. 83 (3) (2000) 461–487.
[3] M.Z.C. Hu, R.D. Hunt, E.A. Payzant, C.R. Hubbard, J. Am. Ceram. Soc. 82 (9) (1999) 2313–2320.
[4] R.E. JuaÂrez, D.G. Lamas, A. Caneiro, N.E. WalsoÈ e de Reca, Nanostruct. Mater. 10 (7) (1998) 1199–1207.
[5] R.E. JuaÂrez, D.G. Lamas, G.E. Lascalea, N.E. WalsoÈ e de Reca, J. Eur. Ceram. Soc. 20 (2000) 133–138.
[6] J.C. Ray, R.K. Pati, P. Pramanik, Mater. Lett. 48 (2001) 74–80.
[7] J.C. Ray, C.R. Saha, P. Pramanik, J. Euro. Ceram. Soc. 22 (2002) 851–862.
[8] J. Yang, J. Lian, Q. Dong, Q. Guan, J. Chen, Z. Guo, Mater. Lett. 57 (2003) 2792–2797.
[9] O. Yamamoto, Y. Arati, Y. Takeda, N. Imanishi, Y. Mizutani, M. Kawai, Solid State Ionics 79 (1995) 137–142.
[10] Y. Xie, J. Am. Ceram. Soc. 82 (3) (1999) 768–770.
[11] T.I. Politova, J.T.S. Irvine, Solid State Ionics 168 (2004) 153–165.
[12] A. Tsoga, A. Naoumidis, W. Jungen, D. StoÈver, J. Euro. Ceram. Soc. 19 (1999) 907–912.
[13] J. Kim, Y.S. Lin, J. Membr. Sci. 139 (1) (1998) 75–83.
[14] G. Dell'Agli, G. Mascolo, J. Eur. Ceram. Soc. 20 (2000) 139–145.
[15] Y.B. Khollam, A.S. Deshpande, A.J. Patil, H.S. Potdar, S.B. Deshpande, S.K. Date, Mater. Chem. Phys. 71 (2001) 235–241.
[16] Ch. Laberty-Robert, F. Ansart, C. Deloget, M. Gaudon, A. Rousset, Mater. Res. Bull. 36 (2001) 2083–2101.
[17] M. Marinsek, K. Zupan, J. Maèek, J. Power Sources 106 (1–2) (2002) 178–188.
[18] A. Ringuede, J.A. Labrincha, J.R. Frade, Solid State Ionics 141–142 (2001) 549–557.
[19] S.T. Aruna, M. Muthuraman, K.C. Patil, Solid State Ionics 111 (1999) 45–51.
[20] L.C. Pathak, T.B. Singh, S. Das, A.K. Verma, P. Ramachandrarao, Mater. Lett. 57 (2002) 380–385.
[21] S. Ramanathan, M.B. Kakade, S.K. Roy, K.K. Kutty, Ceram. Int. 29 (5) (2003) 477–484.
[22] S.R. Jain, K.C. Adiga, V.R. Pai Verneker, Combust. Flame 40 (1981) 71–79.
[23] P. McCarthy, JCPDS 30-1048, Penn. State Univ., Pennsylvania, USA, Grant-in-Aid Report (1977).